sustainability

MDPI

Article

Effect of the C/N Ratio on Biodegradation of Ciprofloxacin and Denitrification from Low C/N Wastewater as Assessed by a Novel 3D-BER System

Mahdi Hassan [1,2], Guangcan Zhu [1,2,*], Zhonglian Yang [1,2], Yongze Lu [1,2], Yan Lang [1,2], Liying Gong [1,2] and Huang Shan [1,2]

1 School of Energy and Environment, Southeast University, Nanjing 210096, China; engrmahdi@gmail.com (M.H.); yangzhonglian@seu.edu.cn (Z.Y.); yzlu@seu.edu.cn (Y.L.); y_yan@seu.edu.cn (Y.L.); lygong@seu.edu.cn (L.G.); 18270911541@163.com (H.S.)

2 State Key Laboratory of Environmental Medicine Engineering of the Ministry of Education, Southeast University, Nanjing 210096, China

* Correspondence: gc-zhu@seu.edu.cn; Tel.: +86-18912966396

Received: 16 August 2020; Accepted: 9 September 2020; Published: 15 September 2020

Abstract: Emerging pollutants in the form of pharmaceuticals have drawn international attention during the past few decades. Ciprofloxacin (CIP) is a common drug widely found in effluents from hospitals, industrial and different wastewater treatment plants, as well as rivers. In this work, the lab-scale 3D-BER system was established, and more than 90% of the antibiotic CIP was removed from Low C/N wastewater. The best results were obtained with the current intensity being taken into account, and a different C/N ratio significantly improved the removal of CIP and nitrates when the ideal conditions were C/N = 1.5–3.5, pH = 7.0–7.5 and I = 60 mA. The highest removal efficiency occurred when CIP = 94.2%, NO_3^--N = 95.5% and total nitrogen (TN) = 84.3%, respectively. In this novel system, the autotrophic-heterotrophic denitrifying bacteria played a vital role in the removal of CIP and an enhanced denitrification process. Thus, autotrophic denitrifying bacteria uses CO_2 and H_2 as carbon sources to reduce nitrates to N_2. This system has the assortment and prosperous community revealed at the current intensity of 60 mA, and the analysis of bacterial community structure in effluent samples fluctuates under different conditions of C/N ratios. Based on the results of LC-MS/MS analysis, the intermediate products were proposed after efficient biodegradation of CIP. The microbial community on biodegrading was mostly found at phylum, and the class level was dominantly responsible for the NO_3^--N and biodegradation of CIP. This work can provide some new insights towards the biodegradation of CIP and the efficient removal of nitrates from low C/N wastewater treatment through the novel 3D-BER system.

Keywords: biodegradation of ciprofloxacin; 3D-BER system; denitrification; microbial communities; low C/N wastewater treatment

1. Introduction

Worldwide, the various kinds of emerging pollutants such as pharmaceuticals compounds, anti-inflammatory drugs, antibiotics, beta-blockers [1] and the massive amount of NO_3^- or NO_2^- have attracted international attention for the last few decades [2]. Shown in Table 1, the antibiotic ciprofloxacin (CIP) is the 3rd-generation fluoroquinolone group usually used in humans and veterinarians [1,3,4]. The high-proportion of CIP is not fully metabolized in livestock and humans, but instead is evacuated as a parent substance [5]. Hence, CIP can reach the environment through various pharmaceutical industries, sewage treatment plants, livestock activities, landfills, application of sewage sludge [6], manure or treated wastewater to agricultural land [3,7,8]. However, due to the potential development

and dissemination of antibiotic resistance, this poses a potential threat to ecosystems and human health [2,3]. Therefore, CIP removal must be considered before being released into the environment [9]. Antibiotic CIP is readily detectable in man-made aquatic-environments (usually found in surface water at ng·L^{-1} to μg·L^{-1} levels) [7]; it occurs at high levels in the effluents of Wastewater Treatment plants (WWTPs) (up to 6.55–31 mg·L^{-1}) receiving pharmaceutical wastewater and rivers polluted with industrial waste (up to 14 mg·L^{-1}) [6,10,11]. During wastewater treatment, 80–90% of CIP was removed by adsorption to sludge, which stabilizes the substance [3].

Some scientific reports and data have shown that biodegradation [7] and the adsorption process [9] were the most effective elimination methods for various kinds of antibiotics in WWTPs [4]. It has been shown in some studies that around 50–100% adsorption is the main path for CIP removal through biodegradation in anaerobic sludge system [12,13]. This clearly shows the importance of sludge being released into the environment as a CIP reservoir and developing sludge management strategies [14]. In general, anaerobic digestion was a standard procedure for the stabilization of sludge; it was also meant to extract organic matter without particular regard for the removal of the antibiotics [8]. The biodegradation rate of absorbent CIP durability was 0–40% during sludge treatment [9,15]. A considerable amount of CIP persisted in the digested sludge contained in wastewater treatment plants [10]. Unfortunately, there were no reports on the microbial community structure of CIP degradation [16,17]. The traditional denitrification process depends on four basic denitrifying enzymes [18] including the respiratory of nitrate reductase [19], which is shown as:

$$NO_3^- \rightarrow NO_2^- \rightarrow NO \rightarrow N_2O \rightarrow N_2$$

However, many processes reported in previous studies were CIP effects on the denitrifying enzymes and the activity of existing denitrifying bacteria [19–21]. In recent years, the biofilm electrode reactors (BERs), which combine biological and electrochemical techniques, have been shown to efficiently eliminate nitrogen, heavy metal and antibiotics [10,22]. The autotrophic denitrify bacteria are immobilized on the cathode surface, and the hydrogen produced from the water-electrolysis is also used as an electron donor in the autotrophic denitrification process [21,22]. Therefore, the anode and cathode materials are typically made of carbon and thus provide an inorganic-carbon source that can be used as a pH buffer solution, as shown in Equations (1)–(3):

$$2H_2O + 2e^- \rightarrow H_2 + 2OH^- \quad (1)$$

$$C + 2H_2 \rightarrow CO_2 + 4H + 4e^- \quad (2)$$

It was shown that the process of denitrification uses hydrogen instead of an organic carbon source [23] to completely covert nitrate to N_2, as per the following reaction [18,24]:

$$2NO_3^- + 5H_2 \rightarrow N_2 + 4H_2O + 2OH^- \quad (3)$$

Since hydrogen is generated from the cathode, it could not cause annoying safety problems, and the dosage was only excessive due to the low solubility of hydrogen [18,24]. The BER only requires an inorganic carbon source [25]. From the literature, the organic-carbon also accumulates in the BERs to enhance the elimination of antibiotics [25,26] and nitrogen through the different C/N ratios [7,27]. The simultaneously heterotrophic-autotrophic bacteria has an improved denitrification process compared to the traditional BER, consumes a large amount of energy and is relatively inefficient [28,29]. We recently introduced a 3D-BER system for the new advanced technique in the potential benefits of low currents, and there is the best capability to treat toxic substances. Hence, effective and economical methods for eliminating CIP antibiotics and nitrate or nitrite were developed. It is also important to improve the methodology to remove the residues of CIP antibiotics that develop when the high manipulative capacity of the anaerobic process occurs in the 3D-BER system.

Table 1. Physical and chemical properties of ciprofloxacin.

Name	Properties	Molecular Formula	Structure
Ciprofloxacin		$C_{17}H_{18}FN_3O_3$	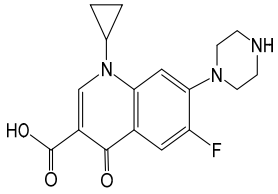
CAS number	85721-33-1		
* *pKa*	10.58 ± 0.30 8.71 ± 0.089 6.14 ± 0.13 3.01 ± 0.30		
* *Log Kow*[b]	0.40		
Molecular weight	331.35 g/mol		

* The pK_a values of ciprofloxacin were obtained from [30], and the value $LogKow^b$ was taken from [31], respectively.

This study demonstrated that the removal efficiency of antibiotics CIP and nitrogen in the effluent of low C/N wastewater can be improved by using a novel 3D-BER system. The primary objectives of this particular study were: (1) to examine the potential toxicity of ciprofloxacin and nitrogen removal; (2) to comprehensively analyze the effect of pH on antibiotics-ciprofloxacin and denitrification; (3) to appraise the degradation by microbial inhabitants and investigate the intermediate product of CIP. Therefore, this is the first study of the removal of CIP to enhance the denitrification process that can be used for solving many problems in low C/N wastewater. As compared to a traditional low C/N ratio in wastewater treatment systems, this technology is also designed to be a more efficient, useful complement or a cost-effective alternative.

2. Materials and Methods

2.1. *Configuration of the* 3D-BER System

The schematic view of the three-dimensional bioelectrochemical reactor system (3D-BERs) was used in this study to evaluate the biodegradation of ciprofloxacin and nitrates removal from Low C/N wastewater (Figure 1). The reactor was made of a plexiglass cylinder with a diameter of 10 cm, a height of 20 cm, a total volume of 1.2 L and a working volume of 0.785 L. The cathode consisting of eight graphite rods (with a height of 20 cm and diameter of 0.8 cm) were placed around the periphery of the reactor, while the one graphite rod (with a height of 20 cm and diameter of 1.5 cm) as an anode was fixed in the center of the reactor and was connected using insulated electrical copper wire by DC-power. A DC-controlled power supply: Model No: HQ3003SIII, supplied by Hansheng Puyuan Technology Beijing Co., Ltd. (Beijing, China), (with the ranges 0–3 A and 0–30 V) was used. Electrolysis of water is the decomposition of water into hydrogen (H_2) and oxygen (O_2) due to the passage of an electric current. Meanwhile, from top to bottom, space was filled with granular activated carbon (GAC) functioning as third particle electrodes (size 1.5–3 mm) used for microbial growth that were purchased from Younga Chemical Technology (Nanjing, Jiangsu Co., Ltd., China). The GAC was the best option for the development of bacteria on the cathode and anode on the inner zone and on the bottom zone in the reactor. The pre-treatment of GAC was washed several times with deionized water via a sulfuric acid solution (0.01 M) and then dried for 24–30 h, and was finally heated to 110 °C.

2.2. *Chemicals and Reagents*

Ciprofloxacin (Analytical-grade > 99%) was obtained from Sigma Aldrich (Munich, Germany). A stock solution of antibiotic CIP (100–500 $\mu g \cdot L^{-1}$) was prepared by using a Milli-Q 18 MΩ system (Millipore, Darmstadt, Germany). The pH was adjusted using 1 M of H_2SO_4 solution prepared with concentrated sulfuric acid (95–97% purity). The high performance liquid chromatography (HPLC) analysis developed by Merck and Fisher was employed with acetonitrile (HPLC quality) and O-phosphate acid (85%). The synthetic wastewater was composed of 30 $mg \cdot L^{-1}$ (NO_3^--N), 3.5 $mg \cdot L^{-1}$ K_2HPO_4, 4.5 $mg \cdot L^{-1}$ NaCl, 5.56 $mg \cdot L^{-1}$ KH_2PO_4, 2.75 $mg \cdot L^{-1}$ $CaCl_2$, 500 $\mu g \cdot L^{-1}$ $C_{17}H_{18}FN_3O_3$ (ciprofloxacin) and 0.1 mL L^{-1} of concentrated trace elements stock solutions, which were prepared by dissolving 1.5 g $MgSO_4$. 7 H_2O, 2.2 g $MnSO_4$. H_2O, 2.2g $ZnSO_4$. H_2O, 0.24 g $CoCl_2$. $6H_2O$, 2 mg

$NiCl_2$. 6 H_2O, 10 mg $FeCl_3$. $6H_2O$, 0.5 mg $CuCl_2$. 2 H_2O, 0.5 mg Na_2MoO_4. H_2O and 1.5 g $CaCl_2$ into 1 L of deionized water [32,33]. Nitrates and antibiotics water effluent samples were filtered by using 0.22-micron membrane filters (Millipore, Darmstadt, Germany) prior to testing. The pH of simulated influent wastewater is typically 7.5 ± 0.2, and no further adjustment was required.

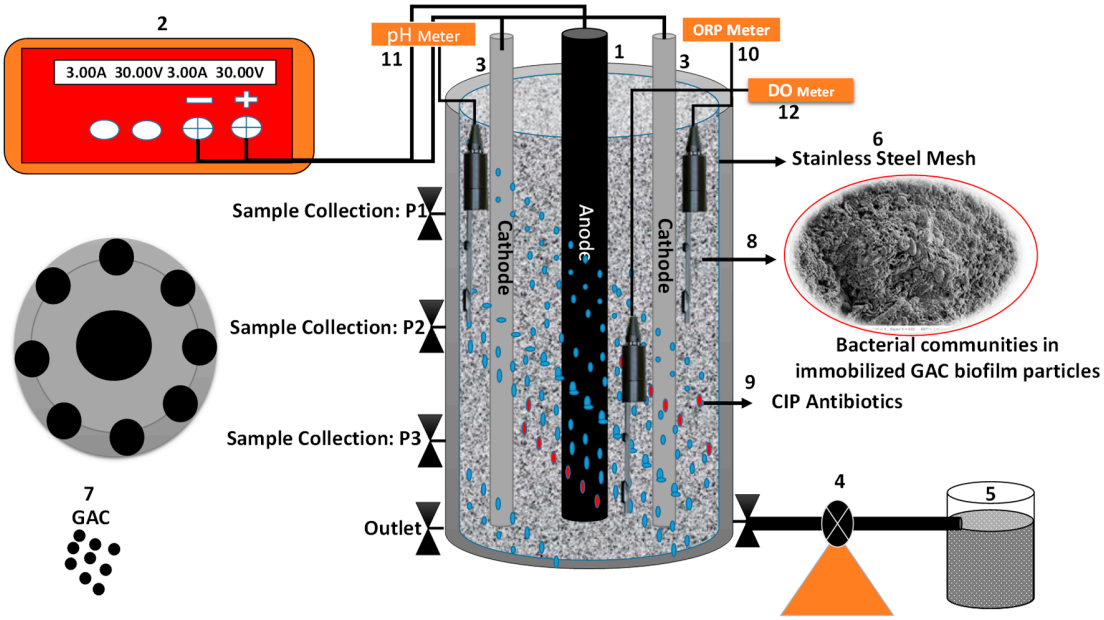

Figure 1. Schematic diagram of the Three-dimensional bioelectrochemical reactor system (3D-BERS) reactor; (1) Graphite anode rod (×1) Size (200 mm × 15 mm); (2) DC regulated power supply; (3) Graphite cathode rods (×8) size (200 × 8 mm); (4) Peristaltic Pump BT300-2J; (5) Influent water tank; (6) Stainless steel mesh; (7) Granular activated carbon (GAC); (8) Bacterial communities in GAC biofilm particles; (9) Ciprofloxacin (CIP) antibiotics; (10) Portable ORP meter model: pH100; (11) Digital pH meter model: pH100; (12) Dissolved meter (DO) model: HI9147. Sample Collection Points (P1, P2, and P3).

2.3. Experimental Procedure

2.3.1. Bacterial Adaptation Phase

All experiments runs were inoculated with a mixed culture of acclimated autotrophic-heterotrophic bacteria (Table 2). These microbes were enriched from the anaerobic sludge (Mixed Liquor Suspended Sludge: MLSS.100 g), which was taken as a bacterial source of inoculation from the Nanjing municipal wastewater treatment plant (WWTP). Before cultivation, 1.2 L of anaerobic sludge water was placed in a refrigerator with nutritious material at 4 °C for seven days. Meanwhile, the synthetic water, which included to NaAc, Nitrates and KH2PO4, was added into the anaerobic sludge with a ratio of C/N/P = 3:1:0.5. During the first three days, sludge water was circulated by a magnetic pump. The concentration of nitrate-nitrogen in the influent was maintained at approximately 30 mg·L−1. After 21 days, anaerobic sludge water was placed in the reactor, and 0.350 L of tap water was added to a total volume of 0.785 L. During the cultivation process, the electrical current was not supplied to the 3D-BER system after two weeks; the direct electrical current was instead gradually adjusted to 10 mA.

Table 2. The initial concentration of Low C/N wastewater at different C/N ratios.

Parameters (mg·L^{-1})	S1	S2	S3	S4	S5	S6	S7
Electric Current (mA)	60	60	60	60	60	60	60
COD	0	15	30	45	75	90	105
NO_3^--N	30	30	30	30	30	30	30
C/N	0	0.5	1.0	1.5	2.5	3.0	3.5

2.3.2. Immobilized GAC Biofilm at Various C/N Ratios

The reactor was started for 70 days of batch operations at an electrically applied current of 60 mA. Each cycle of the 3D-BERs (feed, react, settle, decant) was 40 min. The dissolved oxygen (DO) in the reactor was kept in a range from 1.25 mg·L−1 to less than 0.2 mg·L−1, and the pH was maintained from 7.0 ± 0.5 to 8.0 ± 0.3. The pre-treated sludge was mixing with the ratio of GAC/Sludge of 3:1.5, and was introduced into the cathode and anode layers of the 3D-BERs. For the batch experiments, the biofilm in the anode/cathode surface, as well as the third electrode GAC, turned into dark grey at room temperature (27 ± 1.5 °C). The influent was renewed two times within 24 h due to fast growth microorganism in the reactor. In the 3D-BER system, sustaining an anaerobic condition was needed to expand denitrifying bacteria. By observing the total nitrogen (TN) concentration in the reactor, when TN was exhausted, the residual substrate could be removed, and fresh substrate was fed to the reactor to avoid an endogenous metabolism of the microorganism.

2.3.3. Analytical Methods and Calculations

On a UV-Visible spectrophotometer (Shimadzu UV-1800, Shimadzu, Kyoto, Japan), the nitrate ($N - NO_3^-$), was measured by a UV-spectrophotometric method at wavelength λ = 220–275 × 2 nm. Nitrite ($N - NO_2^-$) was measured by the *N*-(1-naphthyl) ethylenediamine dihydrochloride spectrophotometric method at λ = 540 nm, and total nitrogen (TN). $N - NH_4^+$ was measured by Nessler's reagent colorimetric method using a UV-visible spectrophotometer at λ = 420 nm, respectively [32]. The pH and ORP were measured by a pH100 pH meter, delivered by Shanghai Yoke Instrument Co., Ltd. (Shanghai, China). A thermometer was inserted into the reactor to monitor the temperature during the experiments. All samples were stored at 4 °C prior to the analysis. At least three samples were taken for each test. Current and voltage were recorded every 60 s to control the pH, bacterial metabolism and hydrolysis process. The removal performance of nitrate and CIP antibiotics was calculated based on the percentages of nitrate reduction and CIP as follows in Equations (4) and (5):

$$\text{The removal efficiency of Nitrates reduction } (\%) = \frac{\text{Nitrate in} - \text{Nitrate out}}{\text{Nitrate in}} \times 100 \quad (4)$$

where "in" is the initial concentration of nitrate, and the "out" is the final concentration of nitrate at time *t*.

$$\text{The removal efficiency of CIP reduction } (\%) = \frac{\text{CIP in} - \text{CIP out}}{\text{CIP in}} \times 100 \quad (5)$$

where "in" and "out" are indications of CIP antibiotics concentration in the inlet and the outlet of the 3D-BERS, respectively.

2.4. Ciprofloxacin Concentrations Measurement and By-Products Identification

The CIP detection wavelength was set at 277 nm (fluorescence detection: 240–480 nm), which was determined by using high-performance liquid chromatography (HPLC, Tokyo, Japan) [33]. However, the antibiotics CIP concentrations in the influent were 100 μg·L^{-1} to 500 μg·L^{-1}, respectively. The CIP separation was carried out using a Phenomenex column of asymmetry column, C18 (3.5 μm × 4.6 mm × 250 mm). The mobile phase was composed of acetonitrile and 0.01 mol L^{-1} tetra-n-butyl ammonium bromide ($C_{16}H_{36}BrN$) solution, trimethylamine at pH 3.0 and methanol with a ratio of 88:12 *v/v* at a flow rate of 1.0 mL min^{-1}. The amount and processing time of the injection were 10 μL and 7.244 min, respectively. In the procedure, the reaction solution was extracted with a syringe needle, which was then directly determined by HPLC [33]. The biodegradation of CIP was monitored with mass-spectrometry (SCIEX Triple Quad^{TM} 7500 LC-MS/MS, California, USA). The extracts were analyzed by using a gradient method (0.3 mL L^{-1}) and an Acclaim^{120} column C18 (2.1 × 150 mm × 2 μm) under two mobile phases. In phase A: water containing 0.1% formic acid and, in the meantime, in phase B-acetonitrile. To assess biodegradation products, a thorough analysis of positive and negative ion modes was used. However, the molecular ions observed in positive and negative ions were

subsequently applied in electrospray ionization techniques to provide a chromatographic shape of these putative biodegradation products. To extract LC-MS/MS spectra of the points determined in the final step, high collision energy was exclusively adjusted, and ion chromatographic response intensity was optimized in the range of 45 eV. From the literature, some researchers confirmed that the BES could improve the mechanism of antibiotic removal from the WWTPs due to adsorption techniques, which is a very economical system. The growth medium of the microbial community utilized the energy and C/N source [34,35]. However, the external calibration curve was used to determine the ciprofloxacin antibiotics concentration with a correlation coefficient (R^2 = 0.985).

2.5. DNA Extraction, PCR Amplification, and High-Throughput Sequencing

High-throughput sequencing was performed on original inoculants and immobilized biofilm samples taken from the 3D-BERs (anode/cathode) layers (1.0 g) and effluent (100 mL) after long-term acclimation at different C/N ratios. The names of the biofilm samples were identified as S1, S2, S3, S4, S5, S6 and S7. All samples were stored in −85 °C for 24 h in a freezer before tests. The bacterial genomic DNA was extracted by the PowerSoil DNA® Isolation Kit (Waters, Eschborn, Germany: MOBIO) according to the manufacturer's instructions. The primers 338F (5′-ACTCCTACGGGAGGGAGCAG-3′) and 806R (5′-GGACTACHVGGGTWTCTAAT-3′) was used to amplify the V3–V4 hypervariable regions of the bacteria 16r RNA gene by Macrogen Inc. (Seoul, Korea). The PCR reaction that followed was: Initial denaturation at 98 °C for 1.5 min, denaturation at 98 °C for 30 s, annealing at 50 °C for 30 s and 30 extension cycles at 72 °C for 30 s. PCR reactions occurred in a triplicate 20 µL mixture. The PCR products that appeared, as a result, were extracted from a 2% agarose gel and further purified using the Gene JET DNA Gel extraction Kit (Thermo Scientific ^{TM}, CN: K0691, California, USA). The concentration and purity of DNA were analyzed by the Quanti-Fluor^{TM} St-Fluorometer (Madison, WI, USA). The resulted productions were pooled in equimolar and paired-end sequenced (300 × 2) on an Illumina MiSeq platform (Illumina, San Diego, CA, USA) according to the protocols developed by Beijing Novogene: Genome Sequencing Company Co., Ltd. (Beijing, China). Using this program, we truncated the adapter with low-quality sequences < Q20, and short sequences < 300-bp were trimmed. Disposing of potential chimeric sequences using the Mothur chimeric UCHIME algorithm. The taxonomic classification of the sequences was conducted using the cutting and filtering readings classifier. The observed operational classifiers' richness (OTU), diversity index such as ChaoI and abundance coverage estimator (ACE) were determined by the Mothur function [36,37].

2.6. Biofilms GAC Samples Analysis by SEM

The seven biofilms samples of particle electrodes surface morphology for bacteria in GAC-biofilms were examined by using scanning electron microscopy (SEM) analysis. Prior to SEM analysis, a series of batch experimental sample processing techniques (i.e., fixed, washed, dehydrated, dried, coating, etc.) was applied. About 0.8 g of GAC biofilm samples were placed in a centrifugal tube (C.T) of 10 mL, and 6000 revolutions/separation were conducted over 5 min. Then, the supernatant was removed and mixed with a sediment sample at the bottom of the C.T, following which 7 mL of 2.5% glutaraldehyde was added. We placed the C.T in the refrigerator at 4 °C for 3 to 4 h, and protected the sample. The tube was centrifuged to centrifuge at 6000 rpm for 5 min, to remove the supernatant after the centrifugation process. We then added about 7 mL of ultrapure water to the GAC biofilm sample left at the bottom of the C.T, then used the centrifuge again for 5 min at 6000 rpm, then removed the top liquid. This clean washing was done three times through the centrifugation process [21,38].

For the next stage, we washed the GAC biofilm, dried it and added 7 mL of 20%, 40%, 50%, 70%, 80%, and 90% ethanol each following 10 min periods. Biofilm samples were dehydrated three times, while 7 mL of ethanol (100%) after 15 min each time. Afterwards, a 7 mL blend of ethanol and acetyl (Ethanol: Isoamyl acetate ratio = 1:1) was discharged into the C.T for 15 min. Finally, we placed the 10 mL samples on filter paper and dried them in a vacuum dryer (Mecha-Tech system Ltd., Bristol, UK) for 24 h at a pre-cooling temperature of 10 °C [23,39]. Then the coating (10 nm gold layer)

sample was examined with Hitachi S-4300 FEG-SEM (Bavaria, Germany, Europe), and the images were collected digitally. The SEM images are shown in Figure 2, including the morphology of biofilm attached to granular activated carbon (GAC) particle electrodes in the 3D-BERs. The GAC had a high specific area of about 450–900 m^2 g^{-1} and a porous structure to facilitate the growth of microbial attachment was reported [20,28,40]. The biofilm samples of the S4, S6 and S7 were abundant compared to the S1, S2, S3 and S5, corresponding to the thicker bacterial community at 60 mA [41]. In the S1 to S3 zones, the microbes were reduced in quantity due to lacking electron donors. It was found that in the 3D-BERs with GAC, biofilm was imbedded due to the abundance of microbial activity [40]. This was clearly observed in rod-shaped graphite anode and cathode, which was authentic and common in the other denitrification system [20,42]. There were also giant microbes found, which may be hydrogen-heterotrophic denitrifying bacteria.

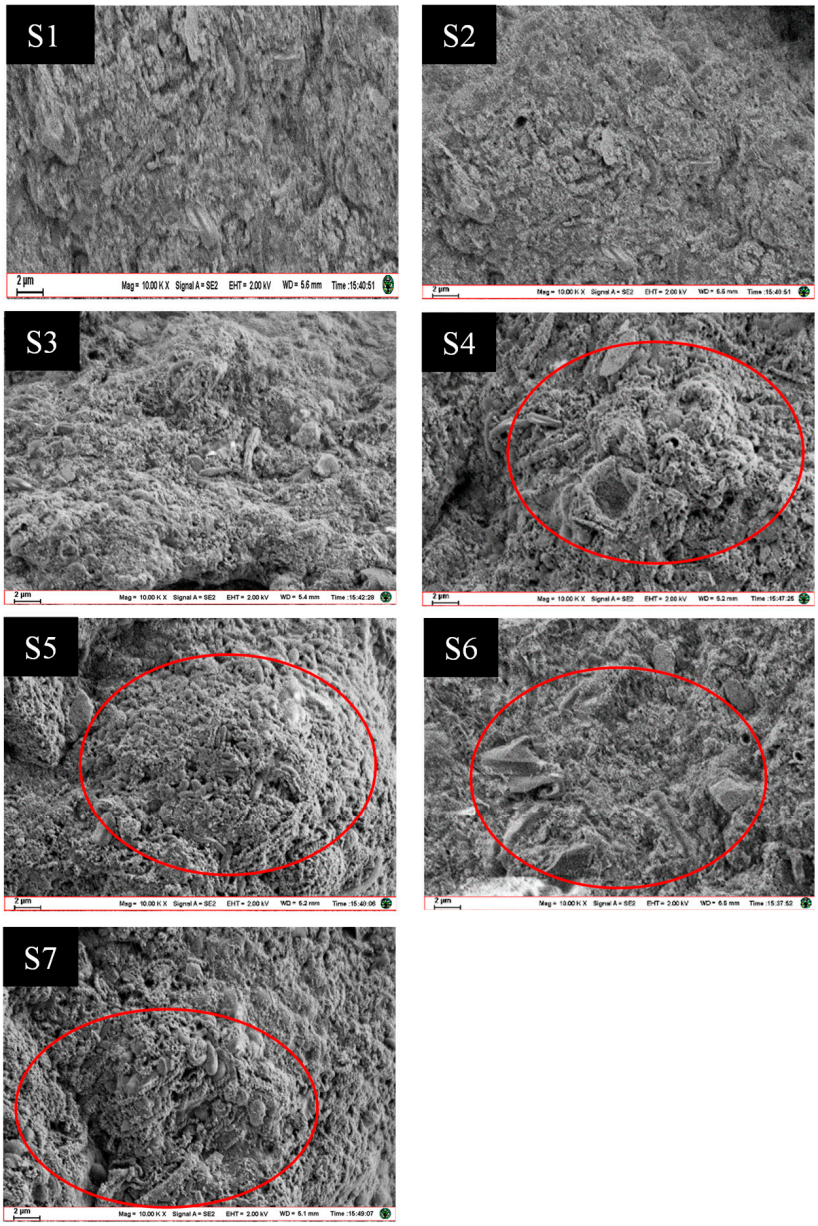

Figure 2. Scanning electron microscopy (SEM) images of GAC biofilm samples of the S4,S5, S6 and S7 were abundant compared to the S1, S2 and S3, corresponding to the vast bacterial community at current intensity of 60 mA in the 3D-BER system.

2.7. Statistical Data Analysis

All effluent samples analytical tests and microbiological analyses in this study were performed twice each time, and the batch test results were obtained by averaging the values of repeated measurements. We used Microsoft Excel (2018) (Microsoft, Redmond, WA, USA) and also used Origin Pro 8.5 and IBM SPSS (v.20) (IBM, Armonk, NY, USA) for the statistical analysis. The final results were expressed as mean ± standard error values, and were considered with statistically significant standards of $p < 0.05$. For all biological studies, seven independent biological tests were performed.

3. Results and Discussion

3.1. Removal Performance and the Effects of C/N Ratios

This analysis shows the average nitrogen concentration (i.e., NO_3^--N, NO_2^--N, NH_3-N, and TN) in the effluent under different C/N ratios during the batch experiments (i.e., I = 60 mA and pH 6.0–8.0), as shown in Figure 3. In the influent, the NO_3^--N concentration remains relatively stable at 30 mg·L^{-1}. When the C/N ratio increases from 0 to 1.5 and 2.5 to 3.5, the average NO_3^--N concentration of the influent falls from 26.09 mg·L^{-1} to 0.9177 mg·L^{-1} and 11.96 mg·L^{-1} to 0.199 mg·L^{-1}, respectively (Figure 3a). Moreover, the NO_3^--N concentration in the final effluent was high when the ideal condition of the C/N ratio was 1.5–3.5, and the final concentration was 0.916 mg·L^{-1}–0.199 mg·L^{-1} as shown in Figure 3c,g. After 30 min, the nitrates concentration dropped rapidly, indicating a significant increase in denitrifying bacteria [19], and that the anoxic condition had been achieved [42]. It was observed that the removal efficiency of nitrogen increased with the amplified C/N ratios.

In particular, the denitrification performance of 3D-BERs with a current intensity of 60 mA was slightly higher in the system as compared with published previous work, as shown in Table 3. When the ratio of C/N increased from 0 to 1.5 and 2.5 to 3.5, the average concentration of total nitrogen in wastewater decreased from 29.26 mg·L^{-1} to 0.955 mg·L^{-1} and from 17.26 mg·L^{-1} to 0.651 mg·L^{-1}, respectively. As shown in Figure 3h, TN average removal efficiency of 3D-BERS was 35.60% to 63.90%, 70.59% to 79.58%, 96.81% to 90.83% and 90.83% to 97.82% when the C/N went from 0 to 0.5, 1 to 1.5, 2.5 to 3.0 and 3.0 to 3.5, respectively ($p < 0.05$) [43,44]. In 3D-BERS, the average removal efficiency was respectively 96.81% and 97.82% when the C/N ratio was 1.5 and 3.5. At the same time, as the ratio of C/N increased from 0 to 1.5 and 2.5 to 3.5, the average NO_2^-N concentration decreased from 2.52 mg·L^{-1} to 0.44 mg·L^{-1} and 1.22 mg·L^{-1} to 0.398 mg·L^{-1}, respectively (Figure 3b). In addition, the C/N ratio was 1.5 and 3.5; the final effluent concentrations respectively were 0.44 mg·L^{-1} and 0.39 mg·L^{-1}. However, under these conditions, the initial NO_3^--N loading of denitrification was high, so NO_2^--N in the wastewater remained at almost zero and was constant [19,43]. Also, the final effluent of NH_3-N in the 3D-BER system decreased from 4.12 mg·L^{-1} to 2.29 mg·L^{-1} and from 4.06 mg·L^{-1} to 1.49 mg·L^{-1}; the different C/N ratios also shifted from 0 to 1.5 and 2.5 to 3.5, and the average NH_3-N concentration in the final effluent was 4.06 mg·L^{-1} to 1.49 mg·L^{-1}, while the C/N ratio was 1.5 to 3.5, in comparison to other techniques previously studied [27,42,43].

Table 3. Comparison from the literature of antibiotic Ciprofloxacin removal and denitrification efficiency with previous studies of BER and 3D-BERS.

Reactor Type	Mode	H/A-D	Treatment Source	E.V (L)	Initial (NO3-N) (mg/L)	C/N Source	Power Source	Input Energy	D.R.R (%)	CIP Removal (%)	Country	References
Three-dimensional bioelectrochemical reactor system (3D-BERS)	Batch	H&A	Synthetic municipal wastewater	0.738	30 mg/L	CH3COONa	DC	60 mA	95.53	94.20	China	This Study
Three-dimensional biofilm-electrode reactor (3D-BER)	Continuous	H&A	Synthetic municipal wastewater	3.4	30 mg/L	CH3CooNa	DC	40 mA	98.3	N/A	China	[18]
Three-dimensional biofilm electrode reactors (3D-BERs)	Batch	A	Synthetic wastewater	2	50–100 mg/L	Hydrogen & α-Fe_2O_3	DC	20–80 mA	95 to 98.9	N/A	China	[20]
A three-dimensional BER	Continuous	H&A	Synthetic groundwater	0.5	20 mg/L	C2H5OH	DC	15mA	100	N/A	China	[22]
Bioelectrochemical System (BES)	Batch	H	Synthetic groundwater	1.0	250 g/m^3 day	CH3CooNa	DC	N/A	14.6 ± 0.2 36.2 ± 5.0	N/A	USA	[25]
A combined single-chamberMFC and BER system	Continuous	H&A	Synthetic groundwater	0.480	364 mg/L	CH3OH	MFC	500–700 mV	30	N/A	China	[37]
A combined BES and sulfur autotrophic denitrification system (CBSAD)	Continuous	A	Synthetic groundwater	33.47	20.9–22.0 mg NO3-N/L	Hydrogen	DC	1000 mA	95	N/A	China	[45]
Bioreactor	Continuous	H&A	Synthetic municipal wastewater	0.9	30 mg/L	C6H12O6	———	———	N/A	20–22	Singapore	[46]
Fe-C micro-electrolysis reactor and up-flow biological aerated filter (UBAF)	Continuous	H&A	Synthetic municipal wastewater	15	60–100 mg/L	Fe-C micro-electrolysis	N/A	N/A	N/A	90	China	[47]

Noted: H/A-D = Heterotrophic /Autotrophic denitrification; DC = Direct Current; E.V = Effective Volume; C/N = Carbon to Nitrogen ratio; D.R.R= Denitrification Removal Rate; CIP = Ciprofloxacin.

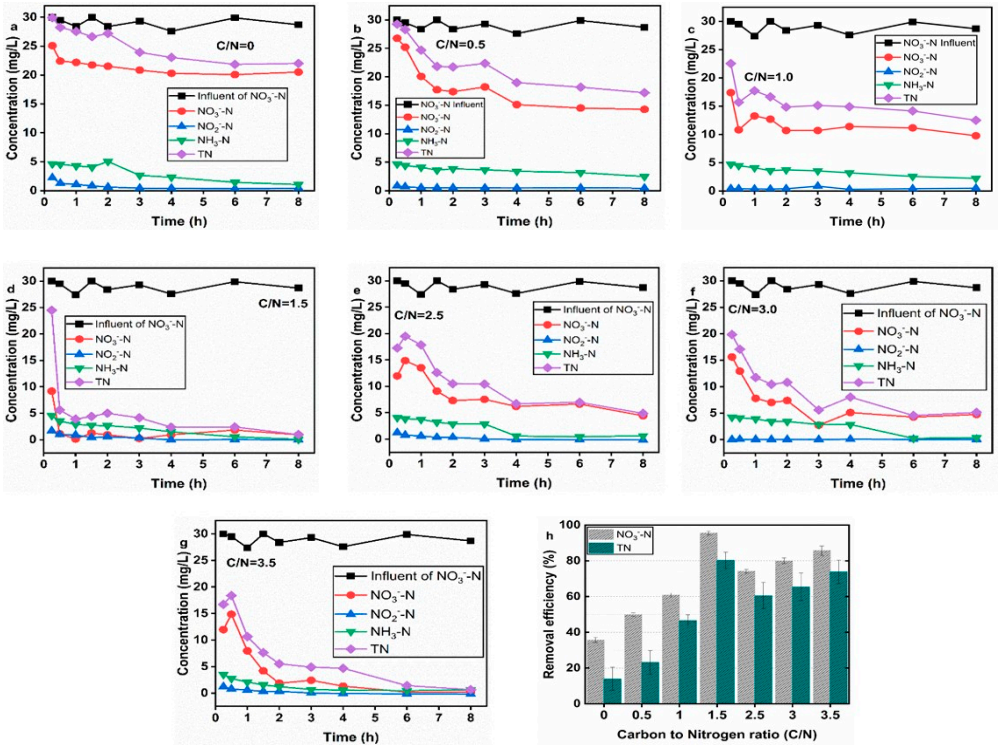

Figure 3. The average effluent concentration of $NO_3^- - N$, $NO_2^- - N$, $NH_3 - N$, TN when the C/N = 0 (**a**), $NO_3^- - N$, $NO_2^- - N$, $NH_3 - N$, TN when the C/N = 0.5 (**b**), $NO_3^- - N$, $NO_2^- - N$, $NH_3 - N$, TN when the C/N=1.0 (**c**), $NO_3^- - N$, $NO_2^- - N$, $NH_3 - N$, TN when the C/N=1.5 (**d**), $NO_3^- - N$, $NO_2^- - N$, $NH_3 - N$, TN when the C/N=2.5 (**e**), $NO_3^- - N$, $NO_2^- - N$, $NH_3 - N$, TN when the C/N=3.0 (**f**), $NO_3^- - N$, $NO_2^- - N$, $NH_3 - N$, TN when the C/N = 3.5 (**g**), and $NO_3^- - N$, TN (**h**) on the denitrification effects and removal efficiency performance under the experimental conditions i.e., I = 60 mA, C/N = 0–3.5, and pH = 5.5–8.0.

Organic carbon sources are known to be limiting factors for heterotrophic denitrification. The removal of nitrate and total nitrogen increases as the ratio of C/N increases [22]. At the maximum level, the C/N ratio endorses the development of heterotrophic-denitrifying microorganisms, thereby allowing denitrification [21,22,47,48]. If there is a shortage of organic carbon during this period, then the nitrogen removal will usually decrease, and the NO_2^--N reductase competes with the electron donor nitrate reductase at a low level of C/N ratio. The reductase of nitrite is more complex and sensitive to the experimental conditions compared to nitrate reductase, resulting in the accumulation of NO_2^--N [22].

Autotrophic denitrifiers were dominated by a low concentration of the C/N ratio required to extend the adaptation period with rapid growth, and had a further accumulation of NO_2^--N [40]. As the C/N ratio increased between 0.5 and 1.5, the effluent NO_2^--N reduced rapidly from 2.52 mg·L^{-1} to 0.242 mg·L^{-1}. At the ratio C/N = 1.5, the NO_2^-—N continues to decline at lower levels. Heterotrophic denitrification may play a pivotal role at an advanced level of the C/N ratio when the rate of denitrification is high. When the C/N ratio was 1.5 and 3.5, the removal efficiency increased by 95.53–85.73% and 80.27–73.85% for NO_3^--N and TN, respectively [49]. However, NH_3-N tends to behave in opposite ways to NO_3^--N and TN. These results are a good comparison with previous findings [19,21,22]. The NO_3^- was commonly used as an acceptor of electrons and could be reduced to NH_4^+ under anoxic and electron-acceptor conditions [20,45].

The 3D-BER system was an anoxic condition, and the force of the electric field prevents NO_3^- from moving to the surface of the anode, so there may be no electron acceptors near the surface of the cathode. In this study, ratio C/N is very close to the complete denitrification in the range of 1.5 to 3.5 and was established by using single heterotrophic denitrification [27,29,50]. Several scientific studies reported

on the elimination of nitrogen were conducted by using autotrophic denitrification [48,51]. Under this method, elimination of NO_3^--N, NH_3-N and total nitrogen increased while the accumulation of NO_2^--N decreased gradually. In this study, the complete denitrification was obtained in C/N = 1.5 and this may be due to the system temperature and denitrification removal rate. However, a similar observation was also reported by other researchers, as shown in Table 3 [40,50].

3.2. *Effects of pH on Antibiotics CIP, Nitrate and Total Nitrogen Removal*

As shown in Figure 4, the influences of various pH values on the average concentration of nitrogen and ciprofloxacin (Total nitrogen, NO_3^--N, and CIP) during the C/N ratio in the batch process from 0 to 3.5 and electrical current intensity was I = 60 mA. A series of batch experiments was conducted in 3D-BERs for 70 days of operation in different C/N ratios to evaluate the NO_3^--N and CIP removal. In the novel 3D-BERs, the elimination of NO_3^--N decreased from 25.07 mg·L^{-1} to 9.18 mg·L^{-1} and from 4.41 mg·L^{-1} to 0.199 mg·L^{-1}, and for CIP there was a reduction from 377.5 µg·L^{-1} to 106.36 µg·L^{-1} and from 115.9 µg·L^{-1} to 106.3 µg·L^{-1} while the C/N was between 0 to 1.5 and 2.5 to 3.5 at the pH range of 6.0 to 7.5 [19,20,40,44]. Under those conditions, the maximum removal efficiencies of NO_3^--N, TN and CIP were found to be 35.66% to 95.55%, 13.93% to 80.27% and 12.59% to 94.20%, while the C/N ratio was between 0 to 1.5 and 2.5 to 3.5 at a electric current intensity of 60 mA, respectively [19,48,52]. The maximum antibiotic CIP removal efficiency could be reached at 84.61% and 94.20% when the C/N was 3.5 and 1.5 at pH values of 7.0 to 7.5. In this system, the highest removal rate was at pH 7.5 as compared to a pH value of 6.7 to 8.0 [37,40]. However, pH played a pivotal role in ciprofloxacin degradation and gradually NO_3^--N removal. It was observed that the average concentration of CIP in influent was decreased from 377 to 106.36 µg·L^{-1} and 115.9 to 116.99 µg·L^{-1} when the C/N ratio shifted from 0 to 1.5 and from 2.5 to 3.5. At the C/N = 1.5 and 3.5, the final effluent of CIP concentrations was 106.36 µg·L^{-1} and 116.99 µg·L^{-1}, respectively, as shown in Figure 5 [50,53,54]. It was shown that denitrification inhibited CIP, and that development was more obvious during the prolonged microbial cultivation period [6,55,56].

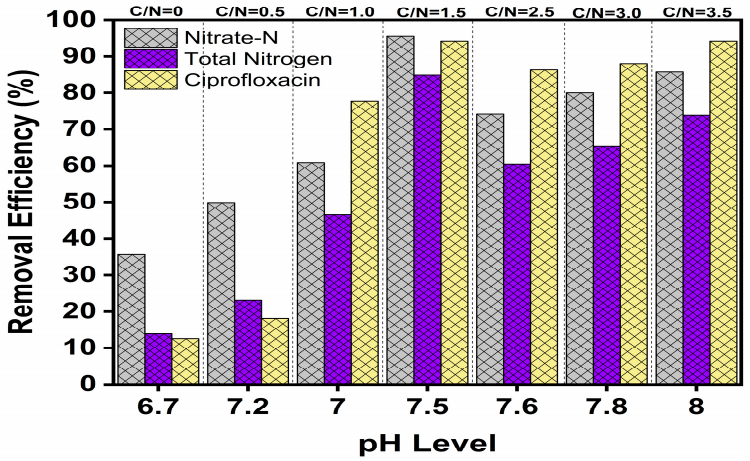

Figure 4. Effects of pH on antibiotics ciprofloxacin and nitrates removal under different pH levels and C/N ratios in the 3D-BER System.

Notably, the pH was an essential factor in the denitrification process and removal of antibiotics. For most denitrifying bacteria, the ideal pH was 7.0–8.2, and previous researchers reported that a pH below 6.0 or 9.0 could indicate immobile heterotrophic and autotrophic denitrification [37,48]. However, when the pH = 7.5, antibiotic CIP, NO_3^--N and total nitrogen (TN) were 106.36 µg·L^{-1}, 0.917 mg·L^{-1} and 0.024 mg·L^{-1}, respectively, and the final effluent amount was the lowest level. The CIP was entirely removed within 16 h of batch experiments at the average removal efficiency of 94.20 ± 0.5%, as reported [10] and observed in this study. Furthermore, the highest average removal

efficiency of CIP, TN and NO_3^--N reached 94.20%, 80.27% and 95.53%, and the enhanced removal efficiency was obtained in 3D-BERS.

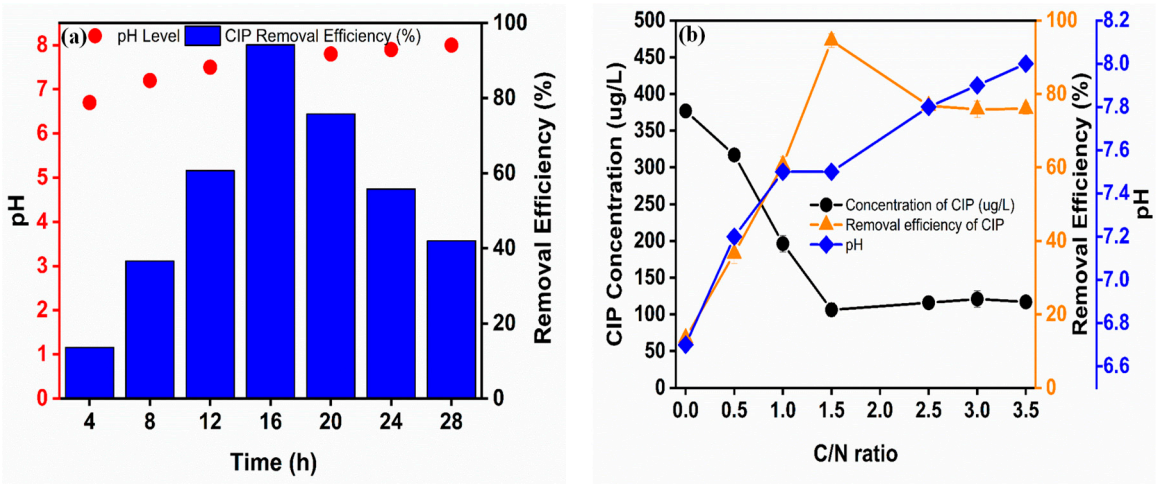

Figure 5. The removal efficiency of (**a**) CIP antibiotics, and (**b**) concentration in the 3D-BERS (i.e., experimental conditions: C/N = 0–3.5, pH = 6.0–8.2).

3.3. Effect of pH on Biodegradation Mechanism of the Antibiotic Ciprofloxacin

Generally, the ideal pH for Autotrophic–Heterotrophic denitrification systems is chosen to be 7.5, because recent reports have shown that increasing antibiotics CIP levels can significantly reduce the performance of autotrophic denitrification systems [6,56]. For another factor that was selected as a variable, the final result under optimal conditions was pH = 7.5. Therefore, the latest novel 3D-BER system was introduced to enhance the denitrification process and achieved the highest removal efficiency for nitrogen. However, Equations (1) and (3) were initiated to indicate that the pH illustrates the OH^- produced during the denitrification process and water electrolysis. In our research work, we found that the pH level of the final effluent was maintained at 7.5 ± 0.2 [51,57]. Moreover, it indicates that the CO_2 produced by the graphite anode not only dissolved in the carbonate but also dissolved in the hydrogen carbonate, as shown in Equation (3), and reacted with OH^-, so that the pH in the following equations is equal to:

$$CO_2 + H_2 \rightarrow H_2CO_3 \quad (6)$$

$$H_2CO_3 + OH^- \rightarrow H_2O + HCO_3^- \quad (7)$$

$$HCO_3^- + OH^- \rightarrow H_2O + CO_3^{2-}. \quad (8)$$

The pH of the system was always in a favourable condition for the biological activity of the denitrifying bacteria. Some scientific research suggests that CIP was predominantly eliminated by adsorption during biological wastewater treatment [7,13]. Previous publications demonstrated that CIP is difficult to manage in regular environments and is hardly degraded by biological processes [9]. Sludge adsorption is the main method to remove ciprofloxacin in wastewater treatment [8,26,46]. Novel research by Li and Zhang et al. showed that there was an initial CIP concentration of 100 $\mu g \cdot L^{-1}$ after 48 h of incubation with a mixture collected from the aeration tank of a biological wastewater treatment plant treated with saline sewage and with a removal capacity of about 32.2% [26]. However, some work on the biodegradation of CIP by biological wastewater treatment processes is significant. The effect of the degradation mechanism of ciprofloxacin antibiotics is affected by changes in the microbial community [9,46,56]. For this research work, the CIP biodegradation was investigated through a series of batch experiments using nitrified sludge anoxic sludge, and the operating system

was 28 h at different C/N ratios. However, the anaerobic sludge is very useful for the biodegradation of CIP, with a concentration of 500 $\mu g \cdot L^{-1}$ in the 3D-BER system.

3.4. Identification of Degradation Pathways by LC-MS/MS

After solid-phase extraction (SPE in Germany), biodegradation experiments on ciprofloxacin antibiotics were performed by using LC-MS/MS. Nevertheless, the LC-MS/MS identified a total of four CIP biotransformation products developed by LC-MS/MS: LCQAD-6460, Agilent Technologies, Santa Clara, CA, USA (the molecular structure and intermediates of these products are revealed in Table S1, and the total ion chromatogram (TIC) is demonstrated in Figure S1). These four possible biodegradation pathways of the antibiotic ciprofloxacin are shown in Figure 6. Moreover, in this pathway, C_2H_2 with a piperazinyl substituent of CIP is removed by using demethylations to generate CIP-BBP1 at the pathway point "S" and is transferred to CIP-BBP4 at the conduit point "Q" by the loss of the C_2H_5N fragment of CIP-BBP1 (Table S1). While the biodegradation of CIP intermediates products involved CIP-BBP1 and CIP-BBP4 as previously reported [16,58], similar products were also identified in 3D-BERS. In the first time of this study, these products were investigated and have not been listed in the literature. In the pathway at point "S", CIP-BBP1 is shaped via hydroxylation (-OH) at the CIP-BBP1-S position, and CIP-BBP4 is also shaped via hydroxylation at the CIP-BBP4-Q position by replacing the piperazinyl group of CIP-BBP1with CIP-BBP4, as presented in Table S1. In the P and Q-points pathways, CIP-BBP2 and CIP-BBP4 were investigated by substituting for both the fluorine at the P-position of CIP [15] and the carboxyl group at the Q-position of CIP with hydroxylation. Meanwhile, the biodegradation of CIP by acetylation of the NH group of piperazine rings caused inactivation of enzyme culture, i.e., it caused the CIP-acetylation process [59]. Therefore, the 4-pathways can be divided into two main reactions: Piperazinyl-substituent decomposition reactions (a), and hydroxylation reactions (b). Figure S1 indicated that the biodegradation mechanism of antibiotic CIP was proposed in the 3D-BER system. Almost all CIP can be converted into the four products mainly through degradation and hydroxylation of the piperazinyl substituent.

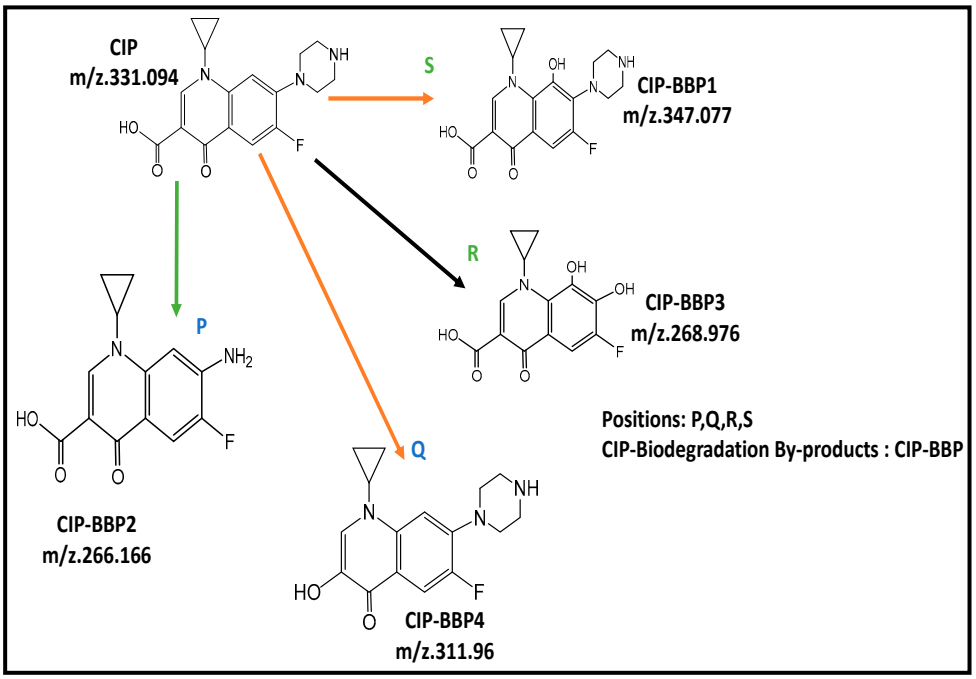

Figure 6. Proposed chemical structure of intermediate products and possible pathways of CIP biodegradation in the novel 3D-BERS by LC-MS/MS.

Pearson's bivariate correlation analysis results showed that CIP biodegradation was significantly correlated in SPSS ($p < 0.01$, $R^2 = 0.996$). To better describe the CIP metabolic degradation pathways [4,23]

at the gene and predominant enzyme levels, superior isolates of ciprofloxacin in anaerobic sludge can be used, as has been indicated by transcriptomics and metagenomics studies [31,59]. The information obtained from LC-MS/MS was insufficient to fully characterize the chemical structure of these metabolites. As a result, realistic standards will be used in future work to confirm the formation of Ciprofloxacin biotransformation pathways.

3.5. Bacterial Diversity and Community Composition

The evolution of ciprofloxacin degradation and denitrifying bacteria both occur after long-term acclimation to low C/N wastewater. Table 4 summarizes the microbial species richness and diversity indices for these two samples. Figure 7 illustrates the phylogenetic classification of phylum and class level sequences for the two main samples in different batch operations. *Proteobacteria, Bacteroidetes* and *Firmicutes* were identified as predominant phyla in seven samples, but their relative abundance was different in each sample (Figure 7A). However, examination of all of the samples showed that the bacteria which dominated in the samples S4 and S7 were more abundant in those samples than in the other samples. The abundance of *Proteobacteria* was the highest out of the different phyla in every sludge sample, and accounted for 48.35%, 51.29%, 61.35%, 95.53%, 71.35%, 78.91% and 83.71%, respectively, of total phyla content in each sample, which is why it was considered to be the main phylum of autotrophic-heterotrophic denitrifying bacteria.

Table 4. Diversity indices of bacterial communities in different sludge samples of 3D-BERS at different C/N ratios and with ab applied electric current of 60 mA.

Condition (C/N)	Sample ID	No. of Reads	No.of OTUs	ACE	Shannon	Simpson	Chao1	Coverage
0	S1	39,322	182	254.321	2.642	0.321	254.119	0.993
0.5	S2	40,215	189	259.583	2.997	0.224	245.337	0.995
1.0	S3	41,234	254	288.981	3.456	0.423	288.327	0.996
1.5	S4	73,382	382	390.705	6.367	0.838	399.229	0.999
2.5	S5	54,633	267	297.149	3.994	0.455	345.657	0.994
3.0	S6	59,236	263	311.597	4.214	0.754	358.279	0.995
3.5	S7	63,324	353	363.642	5.247	0.936	361.571	0.999

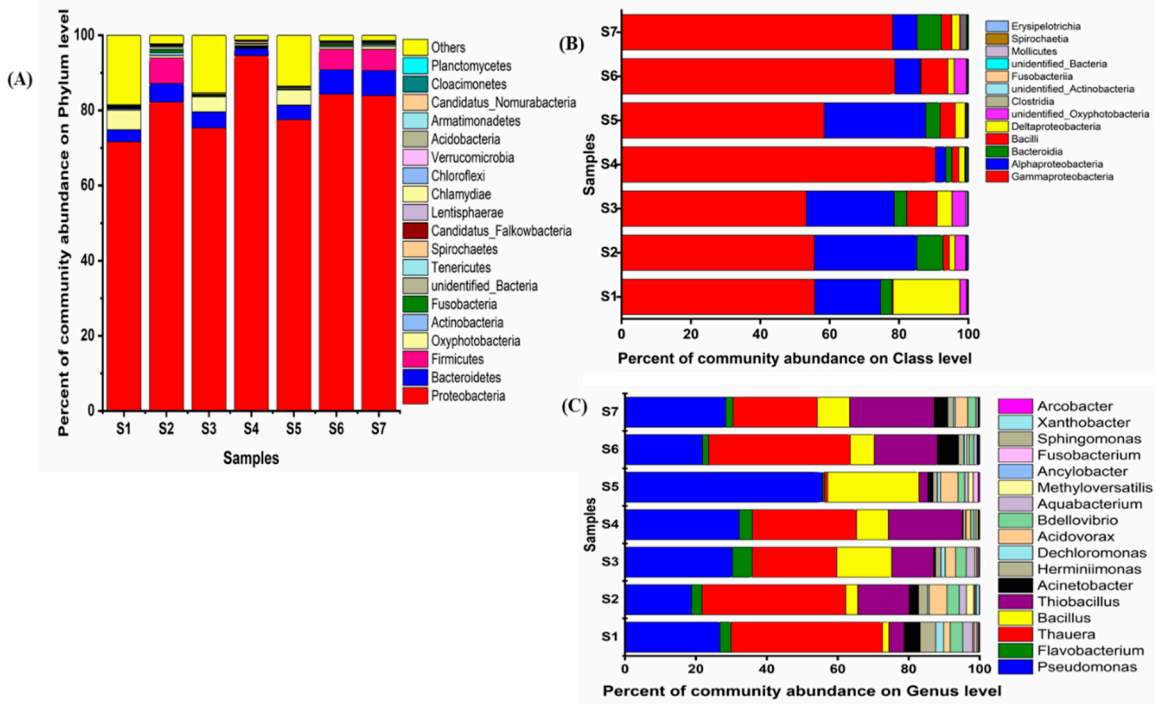

Figure 7. Bacterial community composition of relative abundance at (**A**) phylum, (**B**) class and (**C**) genus levels at different C/N ratios and with a constant electric current I = 60 mA in the 3D-BER system.

It was clearly observed that the richness of *Firmicutes* increased 7 times (raised from 0.011% to 5.63%) when the NO_3^--N concentration increased from 0 to 30 mg/L. *Firmicutes* are generally accepted to have denitrification potential under anaerobic environments, meaning it could survive under extremely oligotrophic conditions by relying on its ability to produce endospores for resisting environment stress.

According to S1 samples of *Firmicutes* (0.011%) obtained was less abundant [15] than the number of S7 samples (5.63%). The relative abundance of class levels is shown in Figure 7B using taxonomic classification.

Furthermore, *Gammaproteobacteria*, *Alphaproteobacteria*, *Bacteroidia*, *Bacillus*, *Deltaproteobacteria* and *Clostridia,* were preponderant classes in sludge samples (Figure 7B). The abundance of *Gammaproteobacteria* accounted for 35.93%, 39.91%, 50.71%, 90.84%, 48.32%, 49.09%, and 74.91% in S1, S2, S3, S4, S5, S6 and S7, respectively, which became the most abundant classes under different C/N ratios.

However, the preponderant classes in the S4 sample were *Alphaproteobacteria* (29.37%), *Gammaproteobacteria* (90.84%), *Bacteroidia* (1.87%), *Deltaproteobacteria* (4.17%), *Bacilli* (8.34%) and *Clostridia* (0.014%) [2,49,59]. It was evident that the distribution of the main classes in these seven samples was significantly different. Nevertheless, the amount of *Gammaproteobacteria* present in sample S4 was more significant than that of any other samples compared to the distribution of *Alphaproteobacteria*, *Bacteroidia*, *Deltaproteobacteria, Bacillus*, *Actinobacteria,* and *Clostridia* [1,3,44]. The equivalent distributions of anaerobic sludge in the S1, S2, S3 and S5 samples were relatively low compared to for the samples S4, S6 and S7 from the 3D-BER system.

It is important to note that the similarities across some variations of S1 to S7 samples shown in Figure 7C indicate the genus levels of more than 65 abundant genera. For any abundant genus with a relative richness of more than 2.5%, the abundance of *Pseudomonas* was significantly higher in the sample S4 (75.34%) when the C/N ratio was 1.5 [9]. In comparison, the relative abundance of *Pseudomonas* in the sample S1 was only 11.44%, while the C/N ratio was 0.5 [4,56]. In general, this result has been widely found in previous studies focusing on *Pseudomonas and Aeruginosa*, especially in terms of the possibility of denitrification [19,60]. Also, *Pseudomonas stutzeri* [40,61], and the certain type of *Pseudomonas.sp* bacteria belonging to the genus *Pseudomonas.sp C27* has autotrophic and heterotrophic denitrifiers that utilize an assortment of electron donors [39]. As the C/N ratio increases, the impact on the bacteria output involved in autotrophic denitrification and the microbial growth yield of denitrifying autotrophic microbes are smaller than that of heterotrophic bacteria. Despite a gradual increase in the C/N ratio, the denitrifying autohydrogenotrophic bacteria may have been gradually domesticated to become heterotrophic denitrifying bacteria that lead to effective nitrates and to antibiotic CIP elimination [62,63]. Therefore, *Pseudomonas* abundance in sample S4 indicates that an overall similarity greater than 94% with autotrophic and heterotrophic denitrifying species is related to *Pseudomonas* in the occurrence of organic substances and applied electrical currents. Moreover, significantly higher amounts of *Thauera.sp* were detected in sample S4 (6.86%) compared to in sample S1 (0.24%). *Bacillus* (15.52%), *Thiobacillus* (28.8%), *Flavobacterium* (3.81%) [4] and *Acinetobacter* (9.59%) are the most important genus of S4 samples, but the abundance for the S7 example involved *Thiobacillus* (23.34%), *Bacillus* (5.6%), *Acinetobacter* (4.53%) and *Flavobacterium* (0.99%) [2,47]. *Thiobacillus* has been identified as a widespread autotrophic bacterium in recent years, closely related to the oxidation of nitrates to nitrogen [39,51]. In recent years, several species belonging to the genera *Thiobacillus, Bacillus* and *Thauera* have been suggested to play an important role in antibiotic CIP and removal of nitrates [56]. Notably, *Thiobacillus* and *Thauera* can transfer electrons directly from the carbon electrode and promote nitrate reduction [16,49,59]. The richness and abundance of *Pseudomonas* (55.04%), *Thiobacillus* (28.88%) and *Thauera* (6.68%) [24,64] were enriched in the 3D-BER system. The removal of CIP and nitrates was due to the distinction between the dominant *Thauera, Pseudomonas* and *Thiobacillus,* which helped to merge heterotrophic denitrification and autotrophic denitrification processes. In conclusion, the main bacteria enhanced in the third electrode (GAC) continues to be

enhanced in both heterotrophic-autotrophic denitrifications, whereas enriched bacteria in S1 are primarily involved in autotrophic denitrification. Therefore, further research is needed to characterize the denitrifying bacteria in the 3D-BER system.

4. Conclusions

Satisfactory antibiotic ciprofloxacin and nitrates removal efficiency was achieved in a novel 3D-BER system from Low C/N wastewater. This system has proved to be more economically and technically attractive than traditional denitrification systems due to the more than 90% reduction of antibiotics and a 55% reduction of sludge production that it causes. Perhaps some resistant bacteria could be used along with antibiotic CIP or dead biomass as an organic substrate for better growth of microbial activities in an anaerobic condition. The microbial community on biodegrading was enriched with a high richness of *Pseudomonas* (75.44%), making it capable of autotrophic-heterotrophic denitrification, although it also contains *Thiobacillus* (48.88%) and *Bacillus* (21.05%) predominant autotrophic bacteria. Biological degradation was the main mechanism for removing CIP and NO_3^--N or NO_2^--N and TN, with few intermediate products detected. Furthermore, this reactor configuration represents a low-cost form of deployment, operation and maintenance technology, compared to other systems and advanced 3D-bioelectrochemical treatment systems.

Supplementary Materials: The following are available online at http://www.mdpi.com/2071-1050/12/18/7611/s1, Figure S1: Mass spectra of biodegradation of ciprofloxacin: Ciprofloxacin (m/z = 331.094) and by-products: CIP-BBP1 (m/z = 331.094); CIP BBP2 (m/z = 266.166); CIP-BBP3 (m/z = 268.976); CIP-BBP4 (m/z = 311.96), Table S1: Antibiotics Ciprofloxacin postulated biodegradation metabolites in 3D-BERS, as determined by HPLC-LC-MS/MS.

Author Contributions: M.H.: formal analysis, data curation, investigation, methodology, writing—original draft, Writing-review—editing. G.Z.: funding acquisition, supervision, project administration, investigation, resources. Z.Y. (Zhonglian Yang): project administration, validation. Y.L. (Yongze Lu): investigation, writing—review—editing. Y.L. (Yan Lang): revised this article critically to assess important intellectual facts. L.G.: investigation, data curation, review—editing. H.S. (Huang Shan): agreed to be held accountable for all aspects of the work and also revised the manuscript. All authors have read and agreed to the published version of the manuscript.

Funding: This research and APC was funded by the National Natural Science Foundation of China under the grant No.51578132.

Conflicts of Interest: The authors declare no conflict of interest.

References

1. Pan, L.-J.; Li, J.; Li, C.-X.; Tang, X.-D.; Yu, G.-W.; Wang, Y. Study of ciprofloxacin biodegradation by a *Thermus* sp. isolated from pharmaceutical sludge. *J. Hazard. Mater.* **2018**, *343*, 59–67. [CrossRef] [PubMed]
2. Meng, F.; Gao, G.; Yang, T.-T.; Chen, X.; Chao, Y.; Na, G.; Ge, L.; Huang, L.-N. Effects of fluoroquinolone antibiotics on reactor performance and microbial community structure of a membrane bioreactor. *Chem. Eng. J.* **2015**, *280*, 448–458. [CrossRef]
3. Nguyen, T.-T.; Bui, X.-T.; Dang, B.-T.; Ngo, H.-H.; Jahng, D.; Fujioka, T.; Chen, S.-S.; Dinh, Q.-T.; Nguyen, C.-N.; Nguyen, T.-T. Effect of ciprofloxacin dosages on the performance of sponge membrane bioreactor treating hospital wastewater. *Bioresour. Technol.* **2019**, *273*, 573–580. [CrossRef] [PubMed]
4. Liao, X.; Li, B.; Zou, R.; Dai, Y.; Xie, S.; Yuan, B. Biodegradation of antibiotic ciprofloxacin: Pathways, influential factors, and bacterial community structure. *Environ. Sci. Pollut. Res.* **2016**, *23*, 7911–7918. [CrossRef] [PubMed]
5. Li, Z.; Hong, H.; Liao, L.; Ackley, C.J.; Schulz, L.A.; Macdonald, R.A.; Mihelich, A.L.; Emard, S.M. A mechanistic study of ciprofloxacin removal by kaolinite. *Colloids Surf. B Biointerfaces* **2011**, *88*, 339–344. [CrossRef]
6. Liu, Z.; Sun, P.; Pavlostathis, S.G.; Zhou, X.; Zhang, Y. Inhibitory effects and biotransformation potential of ciprofloxacin under anoxic/anaerobic conditions. *Bioresour. Technol.* **2013**, *150*, 28–35. [CrossRef]
7. Sahlin, S.; Joakim Larsson, D.; Ågerstrand, M. Ciprofloxacin: EQS Data Overview. In *The Department of Environmental Science and Analytical Chemistry (ACES) Report*; Stockholms Universitet: Stockholm, Sweden, 2018; p. 15.

8. Mougin, C.; Cheviron, N.; Repincay, C.; Hedde, M.; Hernandez-Raquet, G. Earthworms highly increase ciprofloxacin mineralization in soils. *Environ. Chem. Lett.* **2013**, *11*, 127–133. [CrossRef]
9. Liu, Z.; Sun, P.; Pavlostathis, S.G.; Zhou, X.; Zhang, Y. Adsorption, inhibition, and biotransformation of ciprofloxacin under aerobic conditions. *Bioresour. Technol.* **2013**, *144*, 644–651. [CrossRef]
10. Lima, V.B.; Goulart, L.A.; Rocha, R.S.; Steter, J.R.; Lanza, M.R. Degradation of antibiotic ciprofloxacin by different AOP systems using electrochemically generated hydrogen peroxide. *Chemosphere* **2020**, *247*, 125807. [CrossRef]
11. Li, J.; Cheng, W.; Xu, L.; Strong, P.; Chen, H. Antibiotic-resistant genes and antibiotic-resistant bacteria in the effluent of urban residential areas, hospitals, and a municipal wastewater treatment plant system. *Environ. Sci. Pollut. Res.* **2015**, *22*, 4587–4596. [CrossRef]
12. Polesel, F.; Lehnberg, K.; Dott, W.; Trapp, S.; Thomas, K.V.; Plósz, B.G. Factors influencing sorption of ciprofloxacin onto activated sludge: Experimental assessment and modelling implications. *Chemosphere* **2015**, *119*, 105–111. [CrossRef] [PubMed]
13. Shokoohi, R.; Ghobadi, N.; Godini, K.; Hadi, M.; Atashzaban, Z. Antibiotic detection in a hospital wastewater and comparison of their removal rate by activated sludge and earthworm-based vermifilteration: Environmental risk assessment. *Process Saf. Environ. Prot.* **2020**, *134*, 169–177. [CrossRef]
14. Sukul, P.; Spiteller, M. *Fluoroquinolone Antibiotics in the Environment. Reviews of Environmental Contamination and Toxicology*; Springer: Berlin/Heidelberg, Germany, 2007; pp. 131–162.
15. Alexandrino, D.A.; Mucha, A.P.; Almeida, C.M.R.; Gao, W.; Jia, Z.; Carvalho, M.F. Biodegradation of the veterinary antibiotics enrofloxacin and ceftiofur and associated microbial community dynamics. *Sci. Total. Environ.* **2017**, *581*, 359–368. [CrossRef] [PubMed]
16. Amorim, C.L.; Moreira, I.S.; Maia, A.S.; Tiritan, M.E.; Castro, P.M. Biodegradation of ofloxacin, norfloxacin, and ciprofloxacin as single and mixed substrates by Labrys portucalensis F. *Appl. Microbiol. Biotechnol.* **2014**, *98*, 3181–3190. [CrossRef] [PubMed]
17. Wang, Z.; Yang, Y.; Dai, Y.; Xie, S. Anaerobic biodegradation of nonylphenol in river sediment under nitrate-or sulfate-reducing conditions and associated bacterial community. *J. Hazard. Mater.* **2015**, *286*, 306–314. [CrossRef]
18. Hao, R.; Li, S.; Li, J.; Meng, C. Denitrification of simulated municipal wastewater treatment plant effluent using a three-dimensional biofilm-electrode reactor: Operating performance and bacterial community. *Bioresour. Technol.* **2013**, *143*, 178–186. [CrossRef]
19. Tao, M.; Guan, L.; Jing, Z.; Tao, Z.; Wang, Y.; Luo, H.; Wang, Y. Enhanced denitrification and power generation of municipal wastewater treatment plants (WWTPs) effluents with biomass in microbial fuel cell coupled with constructed wetland. *Sci. Total. Environ.* **2020**, *709*, 136159. [CrossRef]
20. Wang, S.-Y.; Yang, X.-Y.; Meng, H.-S.; Zhang, Y.-C.; Li, X.-Y.; Xu, J. Enhanced denitrification by nano α-e_2O_3 induced self-assembled hybrid biofilm on particle electrodes of three-dimensional biofilm electrode reactors. *Environ. Int.* **2019**, *125*, 142–151. [CrossRef]
21. Zhao, Y.; Zhang, B.; Feng, C.; Huang, F.; Zhang, P.; Zhang, Z.; Yang, Y.; Sugiura, N. Behavior of autotrophic denitrification and heterotrophic denitrification in an intensified biofilm-electrode reactor for nitrate-contaminated drinking water treatment. *Bioresour. Technol.* **2012**, *107*, 159–165. [CrossRef]
22. Zhou, M.; Fu, W.; Gu, H.; Lei, L. Nitrate removal from groundwater by a novel three-dimensional electrode biofilm reactor. *Electrochim. Acta* **2007**, *52*, 6052–6059. [CrossRef]
23. Gros, H. Biological denitrification process with hydrogen-oxidizing bacteria for drinking water treatment. *Water Supply* **1988**, *6*, 193–198.
24. Kurt, M.; Dunn, I.J.; Bourne, J.R. Biological denitrification of drinking water using autotrophic organisms with H2 in a fluidized-bed biofilm reactor. *Biotechnol. Bioeng.* **1987**, *29*, 493–501. [CrossRef] [PubMed]
25. Tong, Y.; He, Z. Nitrate removal from groundwater driven by electricity generation and heterotrophic denitrification in a bioelectrochemical system. *J. Hazard. Mater.* **2013**, *262*, 614–619. [CrossRef] [PubMed]
26. Li, B.; Zhang, T. Biodegradation and adsorption of antibiotics in the activated sludge process. *Environ. Sci. Technol.* **2010**, *44*, 3468–3473. [CrossRef] [PubMed]
27. Sobieszuk, P.; Szewczyk, K. Estimation of (C/N) ratio for microbial denitrification. *Environ Technol.* **2006**, *27*, 103–108. [CrossRef] [PubMed]
28. Park, H.I.; Kim, J.S.; Kim, D.K.; Choi, Y.-J.; Pak, D. Nitrate-reducing bacterial community in a biofilm-electrode reactor. *Enzym. Microb. Technol.* **2006**, *39*, 453–458. [CrossRef]

29. Percheron, G.; Bernet, N.; Moletta, R. Interactions between methanogenic and nitrate reducing bacteria during the anaerobic digestion of an industrial sulfate rich wastewater. *FEMS Microbiol. Ecol.* **1999**, *29*, 341–350. [CrossRef]
30. Wei, X.; Chen, J.; Xie, Q.; Zhang, S.; Ge, L.; Qiao, X. Distinct photolytic mechanisms and products for different dissociation species of ciprofloxacin. *Environ. Sci. Technol.* **2013**, *47*, 4284–4290. [CrossRef]
31. Ji, Y.; Ferronato, C.; Salvador, A.; Yang, X.; Chovelon, J.-M. Degradation of ciprofloxacin and sulfamethoxazole by ferrous-activated persulfate: Implications for remediation of groundwater contaminated by antibiotics. *Sci. Total. Environ.* **2014**, *472*, 800–808. [CrossRef]
32. Hamilton, E. Laboratory manual for the examination of water, waste water and soil. *Sci. Total Environ.* **1990**, *92*, 289. [CrossRef]
33. Guo, H.; Jiang, N.; Wang, H.; Shang, K.; Lu, N.; Li, J.; Wu, Y. Pulsed discharge plasma induced WO3 catalysis for synergetic degradation of ciprofloxacin in water: Synergetic mechanism and degradation pathway. *Chemosphere* **2019**, *230*, 190–200. [CrossRef] [PubMed]
34. Hijosa-Valsero, M.; Fink, G.; Schlüsener, M.P.; Sidrach-Cardona, R.; Martín-Villacorta, J.; Ternes, T.; Becares, E. Removal of antibiotics from urban wastewater by constructed wetland optimization. *Chemosphere* **2011**, *83*, 713–719. [CrossRef] [PubMed]
35. Dorival-García, N.; Zafra-Gómez, A.; Navalón, A.; González, J.; Vilchez, J. Removal of quinolone antibiotics from wastewaters by sorption and biological degradation in laboratory-scale membrane bioreactors. *Sci. Total Environ.* **2013**, *442*, 317–328. [CrossRef] [PubMed]
36. Chen, D.; Wang, H.; Yang, K.; Ma, F. Performance and microbial communities in a combined bioelectrochemical and sulfur autotrophic denitrification system at low temperature. *Chemosphere* **2018**, *193*, 337–342. [CrossRef]
37. Zhang, B.; Liu, Y.; Tong, S.; Zheng, M.; Zhao, Y.; Tian, C.; Liu, H.; Feng, C. Enhancement of bacterial denitrification for nitrate removal in groundwater with electrical stimulation from microbial fuel cells. *J. Power Sources* **2014**, *268*, 423–429. [CrossRef]
38. Fry, D.E.; Garrison, R.N.; Trachtenberg, L.; Polk, H.C. Bacterial inoculum and the activity of antimicrobial agents. *Surg. Gynecol. Obstet.* **1985**, *160*, 105–108.
39. Chen, C.; Ho, K.-L.; Liu, F.-C.; Ho, M.; Wang, A.-J.; Ren, N.; Lee, D.-J. Autotrophic and heterotrophic denitrification by a newly isolated strain *Pseudomonas* sp. C27. *Bioresour. Technol.* **2013**, *145*, 351–356. [CrossRef]
40. Srivastava, P.; Yadav, A.K.; Abbassi, R.; Garaniya, V.; Lewis, T.W. Denitrification in a low carbon environment of a constructed wetland incorporating a microbial electrolysis cell. *J. Environ. Chem. Eng.* **2018**, *6*, 5602–5607. [CrossRef]
41. Mousavi, S.A.; Ibrahim, S.; Aroua, M.; Ghafari, S. Development of nitrate elimination by autohydrogenotrophic bacteria in bio-electrochemical reactors—A review. *Biochem. Eng. J.* **2012**, *67*, 251–264. [CrossRef]
42. Wu, G.; Li, Z.; Huang, Y.; Zan, F.; Dai, J.; Yao, J.; Yang, B.; Chen, G.; Lei, L. Electrochemically assisted sulfate reduction autotrophic denitrification nitrification integrated (e-SANI®) process for high-strength ammonium industrial wastewater treatment. *Chem. Eng. J.* **2020**, *381*, 122707. [CrossRef]
43. Bertanza, G.; Menoni, L.; Capoferri, G.U.; Pedrazzani, R. Promoting biological phosphorus removal in a full scale pre-denitrification wastewater treatment plant. *J. Environ. Manag.* **2019**, *254*, 109803. [CrossRef] [PubMed]
44. Ge, S.; Ma, J.; Liu, L.; Yuan, Z.-M. The Impact of Exogenous Aerobic Bacteria on Sustainable Methane Production Associated with Municipal Solid Waste Biodegradation: Revealed by High-Throughput Sequencing. *Sustainability* **2020**, *12*, 1815. [CrossRef]
45. Wan, D.; Liu, H.; Qu, J.; Lei, P.; Xiao, S.; Hou, Y. Using the combined bioelectrochemical and sulfur autotrophic denitrification system for groundwater denitrification. *Bioresour. Technol.* **2009**, *100*, 142–148. [CrossRef] [PubMed]
46. Kim, D.; Nguyen, L.N.; Oh, S. Ecological impact of the antibiotic ciprofloxacin on microbial community of aerobic activated sludge. *Environ. Geochem. Heal.* **2019**, *2019*, 1–11. [CrossRef]
47. Zhang, L.; Yue, Q.; Yang, K.; Zhao, P.; Gao, B. Analysis of extracellular polymeric substances (EPS) and ciprofloxacin-degrading microbial community in the combined Fe-C micro-electrolysis-UBAF process for the elimination of high-level ciprofloxacin. *Chemosphere* **2018**, *193*, 645–654. [CrossRef]

48. Zhao, Y.; Feng, C.; Wang, Q.; Yang, Y.; Zhang, Z.; Sugiura, N. Nitrate removal from groundwater by cooperating heterotrophic with autotrophic denitrification in a biofilm–electrode reactor. *J. Hazard. Mater.* **2011**, *192*, 1033–1039. [CrossRef] [PubMed]
49. Song, P.; Huang, G.; Hong, Y.; An, C.; Xin, X.; Zhang, P. A biophysiological perspective on enhanced nitrate removal from decentralized domestic sewage using gravitational-flow multi-soil-layering systems. *Chemosphere* **2020**, *240*, 124868. [CrossRef]
50. Si, Z.; Song, X.; Wang, Y.; Cao, X.; Zhao, Y.; Wang, B.; Chen, Y.; Arefe, A.; Wang, Y. Intensified heterotrophic denitrification in constructed wetlands using four solid carbon sources: Denitrification efficiency and bacterial community structure. *Bioresour. Technol.* **2018**, *267*, 416–425. [CrossRef]
51. Chiu, Y.-C.; Chung, M.-S. Determination of optimal COD/nitrate ratio for biological denitrification. *Int. Biodeterior. Biodegrad.* **2003**, *51*, 43–49. [CrossRef]
52. Yi, K.; Wang, D.; Yang, Q.; Li, X.; Chen, H.; Sun, J.; An, H.; Wang, L.; Deng, Y.; Liu, J.; et al. Effect of ciprofloxacin on biological nitrogen and phosphorus removal from wastewater. *Sci. Total. Environ.* **2017**, *605*, 368–375. [CrossRef]
53. Zhang, H.; Jia, Y.; Khanal, S.K.; Lu, H.; Fang, H.; Zhao, Q. Understanding the Role of Extracellular Polymeric Substances on Ciprofloxacin Adsorption in Aerobic Sludge, Anaerobic Sludge, and Sulfate-Reducing Bacteria Sludge Systems. *Environ. Sci. Technol.* **2018**, *52*, 6476–6486. [CrossRef] [PubMed]
54. Hermosilla, D.; Han, C.; Nadagouda, M.N.; Machala, L.; Gascó, A.; Campo, P.; Dionysiou, D.D. Environmentally friendly synthesized and magnetically recoverable designed ferrite photo-catalysts for wastewater treatment applications. *J. Hazard. Mater.* **2019**, *381*, 121200. [CrossRef] [PubMed]
55. Wang, K.; Gao, D.; Xu, J.; Cai, L.; Cheng, J.; Yu, Z.; Hu, Z.; Yu, J. Interaction of ciprofloxacin with the activated sludge of the sewage treatment plant. *Environ. Sci. Pollut. Res.* **2018**, *25*, 35064–35073. [CrossRef]
56. Kim, D.G.; Choi, D.; Cheon, S.; Ko, S.-O.; Kang, S.; Oh, S. Addition of biochar into activated sludge improves removal of antibiotic ciprofloxacin. *J. Water Process. Eng.* **2020**, 33. [CrossRef]
57. Jiang, M.; Zheng, X.; Chen, Y. Enhancement of denitrification performance with reduction of nitrite accumulation and N2O emission by Shewanella oneidensis MR-1 in microbial denitrifying process. *Water Res.* **2020**, *169*, 115242. [CrossRef] [PubMed]
58. Jia, Y.; Khanal, S.K.; Shu, H.; Zhang, H.; Chen, G.-H.; Lu, H. Ciprofloxacin degradation in anaerobic sulfate-reducing bacteria (SRB) sludge system: Mechanism and pathways. *Water Res.* **2018**, *136*, 64–74. [CrossRef] [PubMed]
59. Girardi, C.; Greve, J.; Lamshöft, M.; Fetzer, I.; Miltner, A.; Schäffer, A.; Kästner, M. Biodegradation of ciprofloxacin in water and soil and its effects on the microbial communities. *J. Hazard. Mater.* **2011**, *198*, 22–30. [CrossRef]
60. Hosono, T.; Alvarez, K.; Lin, I.-T.; Shimada, J. Nitrogen, carbon, and sulfur isotopic change during heterotrophic (*Pseudomonas aureofaciens*) and autotrophic (*Thiobacillus denitrificans*) denitrification reactions. *J. Contam. Hydrol.* **2015**, *183*, 72–81. [CrossRef]
61. Sakakibara, Y.; Araki, K.; Watanabe, T.; Kuroda, M. The denitrification and neutralization performance of an electrochemically activated biofilm reactor used to treat nitrate-contaminated groundwater. *Water Sci. Technol.* **1997**, *36*, 61. [CrossRef]
62. Huo, S.; Kong, M.; Zhu, F.; Qian, J.; Huang, D.; Chen, P.; Ruan, R. Co-culture of Chlorella and wastewater-borne bacteria in vinegar production wastewater: Enhancement of nutrients removal and influence of algal biomass generation. *Algal Res.* **2020**, *45*, 101744. [CrossRef]
63. Stuckey, D.C.; Oh, S. Effect of ciprofloxacin on methane production and anaerobic microbial community. *Bioresour. Technol.* **2018**, *261*, 240–248.
64. Gonzalez-Martinez, A.; Rodriguez-Sanchez, A.; Martinez-Toledo, M.; García-Mesa, J.J.; Hontoria, E.; Osorio-Robles, F.; Gonzalez–Lopez, J. Effect of ciprofloxacin antibiotic on the partial-nitritation process and bacterial community structure of a submerged biofilter. *Sci. Total. Environ.* **2014**, *476*, 276–287. [CrossRef] [PubMed]